Developmental Cell *11*, 483–493, October, 2006 ©2006 Elsevier Inc. DOI 10.1016/j.devcel.2006.08.012

The Agrin/Perlecan-Related Protein Eyes Shut Is Essential for Epithelial Lumen Formation in the *Drosophila* Retina

Nicole Husain,[1] Milena Pellikka,[1] Henry Hong,[1] Tsveta Klimentova,[1] Kwang-Min Choe,[2] Thomas R. Clandinin,[2,3] and Ulrich Tepass[1,4,*]

[1] Department of Cell and Systems Biology
University of Toronto
Toronto, Ontario M5S 3G5
Canada

[2] Department of Neurobiology
Stanford University
Stanford, California 94305

Summary

The formation of epithelial lumina is a fundamental process in animal development. Each ommatidium of the *Drosophila* retina forms an epithelial lumen, the interrhabdomeral space, which has a critical function in vision as it optically isolates individual photoreceptor cells. Ommatidia containing an interrhabdomeral space have evolved from ancestral insect eyes that lack this lumen, as seen, for example, in bees. In a genetic screen, we identified *eyes shut* (*eys*) as a gene that is essential for the formation of matrix-filled interrhabdomeral space. Eys is closely related to the proteoglycans agrin and perlecan and secreted by photoreceptor cells into the interrhabdomeral space. The honeybee ortholog of *eys* is not expressed in photoreceptors, raising the possibility that recruitment of *eys* expression has made an important contribution to insect eye evolution. Our findings show that the secretion of a proteoglycan into the apical matrix is critical for the formation of epithelial lumina in the fly retina.

Introduction

Many internal organs such as lungs, liver, pancreas, and kidneys contain epithelial tubes in which polarized epithelial cells surround a luminal space. Lumen formation and the maintenance of a specific lumen size, shape, and composition are important determinants of organ function. Work on models, such as the branching network of epithelial tubes that constitutes the respiratory (tracheal) system of flies or mammalian epithelial Madin-Darby canine kidney (MDCK) cells grown in a three-dimensional matrix, has begun to illuminate the cellular and molecular mechanisms of tube formation (for reviews, see Hogan and Kolodziej, 2002; O'Brien et al., 2002; Lubarsky and Krasnow, 2003; Affolter et al., 2003). The different strategies that are employed to create tubes hold in common that polarized epithelial architecture of the surrounding cells is either maintained or generated during tube biogenesis so that the lumen is bound by the apical surfaces of those epithelial cells. This suggests that the formation as well as the size, shape, and secretory activity of the apical membrane have pivotal functions in lumen biogenesis.

Formation of epithelial tubes is also an important aspect of nervous system morphogenesis. Neurulation in vertebrates involves the invagination of the neuroepithelium, which gives rise to the neural tube. The lumen of the neural tube can be the direct result of the invagination process or may develop secondarily through cavitation or cord hollowing (Colas and Schoenwolf, 2001). For example, neurulation in zebrafish embryos leads to the formation of a neural keel in which the apical surfaces of opposing neuroepithelial cells are in direct contact so that no lumen is apparent initially. The lumen opens later in development when the apical surfaces retract from each other (Schmitz et al., 1993). Thus, while biogenesis of the apical membrane as a result of epithelial polarization can go hand in hand with lumen formation, both processes may also be separated temporally, indicating that in addition to apical membrane formation other mechanisms are needed to open a luminal cavity. The lumen of the neural tube gives rise to the ventricular space of the adult central nervous system and the subretinal space of the retina, which is bound by the apical surfaces of photoreceptor cells (PRCs) and Müller glia cells on one side and the retinal pigment epithelium on the other. The subretinal space has an important function in vision, as some of its components contribute to the recycling of the photopigment (Gonzalez-Fernandez, 2003).

Each ommatidium of a fly eye contains a luminal space, the interrhabdomeral space (IRS), that has a critical function in vision. The visual system of flies is built following the principle of neural superposition, an architecture that is believed to have evolved from an apposition compound eye type found in most insects (Kirschfeld, 1967; Braitenberg, 1967; Land and Nilsson, 2002). As a consequence, fly eyes are more sensitive to light while retaining the resolving power of an apposition eye with the same number of ommatidia. In apposition eyes, such as those of bees, each ommatidium samples a different area in the visual field. All PRCs within one ommatidium collect light from the same area and their photosensitive membranes, the rhabdomeres, are not required to be optically isolated and tightly adhere to each other at the center of the ommatidium, forming a "fused rhabdome" (Figure 1B). The main PRCs of an ommatidium in apposition eyes (PRCs R2–4 and R6–8 of bees) project axons to the same interneuronal cartridge in the first optic ganglion, the lamina. This eye architecture implies that the sensitivity of apposition eyes is determined by the diameter (the aperture) of a single ommatidium. In contrast, in neural superposition eyes of flies, the main PRCs within each ommatidium (PRCs R1–6 in flies) detect light from different areas in the visual field. This requires two critical morphological changes. First, fly ommatidia display an "open rhabdom," where PRCs are optically isolated from each other, a function provided by the IRS (Figure 1A).

*Correspondence: utepass@zoo.utoronto.ca

[3] Lab address: http://med.stanford.edu/profiles/frdActionServlet?choiceId=facProfile&fid=3885.

[4] Lab address: http://www.csb.utoronto.ca/faculty/index.cfm?fmMode=facultyProfile&prof_id=109.

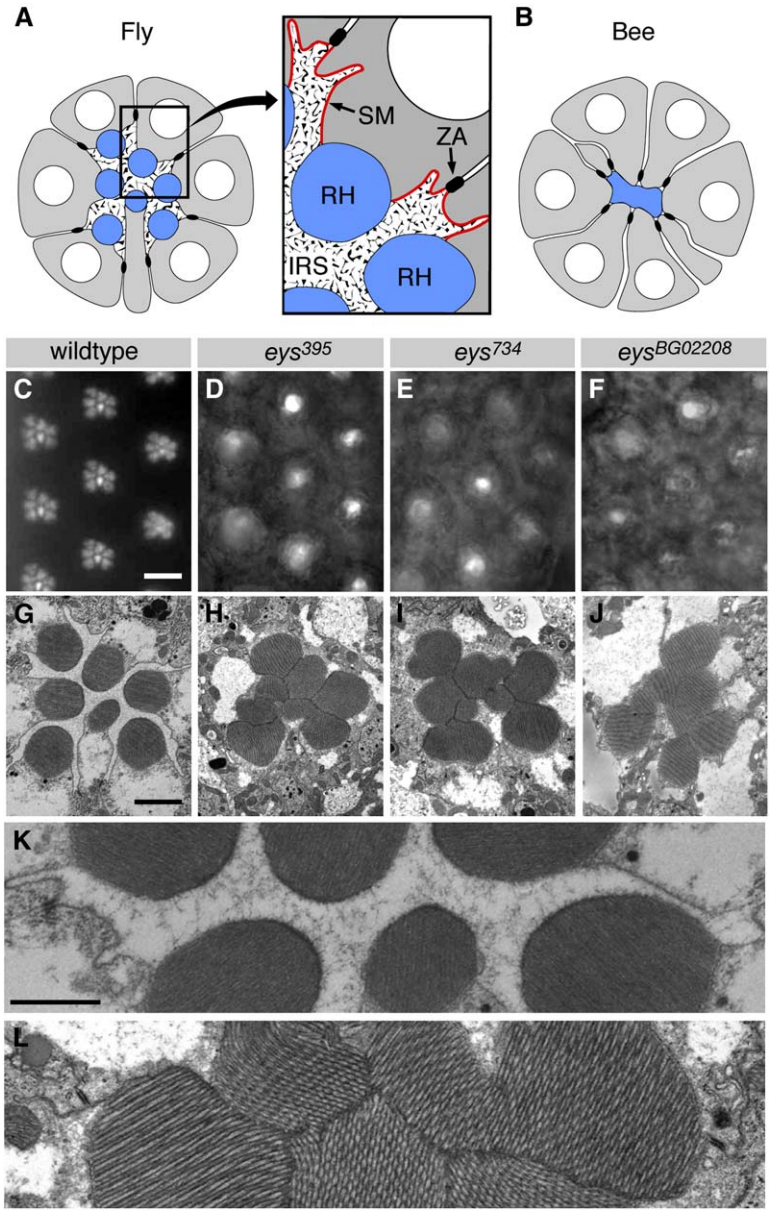

Figure 1. *eys* Is Required for IRS Formation

(A) Schematic illustration of a fly ommatidium in which the PRCs surround a central luminal space. IRS, interrhabdomeral space; RH, rhabdomere; SM, stalk membrane; ZA, zonula adherens.

(B) Schematic illustration of a bee ommatidium in which no IRS is found and all rhabdomeres are in close contact.

(C) Rhabdomeres act as light guides and can be visualized by transmitted light illumination. Individual rhabdomeres of wild-type ommatidia appear separated from each other, as they are optically isolated.

(D–F) *eys* mutants have lost optical isolation of rhabdomeres, as ommatidia display a single dot of transmitted light.

(G–J) Transmission electron micrographs (TEM) of wild-type (G) and *eys* mutant (H–J) ommatidia showing that the IRS is missing in *eys* mutants and rhabdomeres and stalk membranes are in direct contact.

(K) TEM close-up showing the diffuse matrix found in the IRS of fly ommatidia.

(L) TEM close-up showing the absence of IRS and direct contact between rhabdomeres and stalk membranes in an eys^{395} mutant.

The scale bars represent (C–F) 5 μm; (G–J) 1 μm; and (K and L) 0.5 μm.

Second, each PRC projects an axon to a different interneuronal cartridge. Each cartridge still receives input from six PRCs that sample the same area in the visual field, but these PRCs are located in six different neighboring ommatidia. The result of these changes in the structure of the visual system is that the fly eye retains its resolving power—the number of areas sampled in the visual field equals the number of ommatidia—but has a larger aperture, and thus greater sensitivity as each area in the visual field is sampled by six ommatidia rather than one.

A number of factors have been identified in recent years that are involved in shaping epithelial tubes and generating lumina of correct dimensions (Myat and Andrew, 2002; Hemphälä et al., 2003; Jazwinska et al., 2003; Göbel et al., 2004; Wu and Beitel, 2004; Perens and Shaham, 2005; Tonning et al., 2005; Devine et al., 2005; Moussian et al., 2005). However, a coherent view of the mechanisms that control lumen morphogenesis is still missing and, in particular, information about how a luminal cavity is opened up after opposing apical membranes have been established is unknown. Here we use the *Drosophila* retina as a model to address this question. We characterize the expression and function of *eyes shut* (*eys*), a gene required for the formation of the IRS. Eys protein is secreted into the matrix-filled IRS and is essential for the opening of a luminal cavity.

Results

Eys Mutants Fail to Form an Interrhabdomeral Space

In a genetic screen that identified *Drosophila* mutants with a compromised optomotor response (Clandinin et al., 2001), we isolated two mutants that did not display optical isolation of PRCs (Figures 1C–1E). These mutants identified a gene that we named *eyes shut*

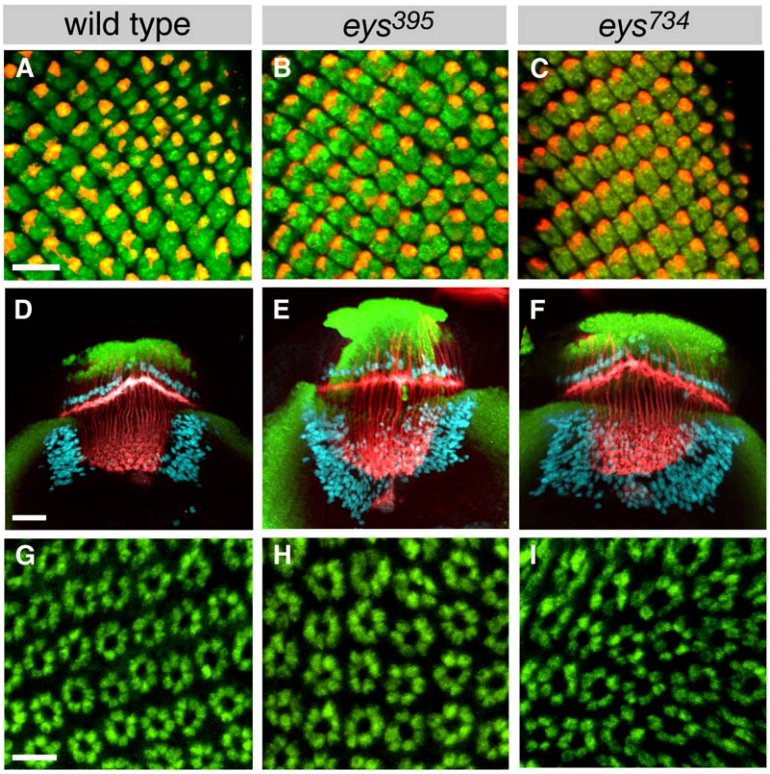

Figure 2. *eys* Mutant PRCs Show Normal Specification and Axonal Connectivity

(A–C) Third larval instar eye discs of wild-type (A), eys^{395}/*Df(2L)BSC37* (B), and eys^{734}/*Df(2L)BSC37* (C) labeled with antibodies directed against Elav (green), a marker of neuronal differentiation, and mδ-lacZ (red), a marker of R4 fate specification, reveal no defects in PRC specification in *eys* mutants.

(D–F) Third larval instar eye-brain complexes of wild-type (D), eys^{395}/*Df(2L)BSC37* (E), and eys^{734}/*Df(2L)BSC37* (F) labeled with antibodies directed against Elav (green), Chaoptin, a PRC-specific antigen (red), and brain-specific homeobox (BSH; blue), a marker for lamina neuron L5, show no defects in the extension of *eys* mutant PRC axons into the brain. At this stage, growth cones of PRCs R1–R6 form a plexus within one optic ganglion, the lamina, while R7 and R8 axons form a retinotopic array of projections in the deeper medulla. Both sets of these projections were unaffected by loss of *eys* activity. The slight disordering of the L5 layer in the lamina is associated with a background mutation on the FRT chromosome, and is not associated with either *eys* or *Df(2L)BSC37* (data not shown).

(G–I) Optical cross-sections of lamina cartridges of wild-type (G), eys^{395}/*Df(2L)BSC37* (H), and eys^{734}/*Df(2L)BSC37* (I) stained with an antibody directed against the presynaptic marker mAb6H4 (green). *eys* mutant PRCs R1–R6 form cartridges indistinguishable from those observed in wild-type brains, indicating that mutant PRCs innervate appropriate postsynaptic targets in the adult brain.

The scale bars represent (A–C) 15 μm; (D–F) 20 μm; and (G–I) 5 μm.

(*eys*; alleles: eys^{395}, eys^{734}). The apical membranes of PRCs that surround the IRS are composed of the rhabdomere and the stalk membrane that links the rhabdomere to the basolateral membrane (Figure 1A). Ultrastructural analysis showed that rhabdomeres and stalk membranes were in close contact in eys^{395} and eys^{734} mutants and individual rhabdomeres were often fragmented (Figures 1G–1I, 1K, and 1L). In some ommatidia of eys^{395} mutants, luminal spaces between stalk membranes were visible but appeared devoid of the diffuse matrix seen in wild-type. Deletion mapping located *eys* in region 22E on chromosome 2L, and examination of local P element insertions identified two additional alleles, $eys^{BG02208}$ and eys^{G13596}, which also prevent IRS formation (Figures 1F and 1J and not shown). Precise excision of $eys^{BG02208}$ reverted the mutant phenotype to wild-type, indicating that the P element insertion was the cause for the *eys* mutation. Imprecise excision gave rise to the mutant allele eys^{PR91}. All allelic combinations are homozygous viable and fertile and showed similar phenotypes in homo- and hemizygosis, suggesting that they are strong loss-of-function or null alleles of *eys*. These findings indicate that *eys* has an essential function in IRS formation.

The second key anatomical feature of neural superposition eyes is the projection of PRC axons from a single ommatidium to different interneuronal cartridges. We therefore examined axonal projections in *eys* mutants and found that they are the same as in wild-type control animals (Figures 2D–2I; see Figure S1 in the Supplemental Data available with this article online). In addition, *eys* mutants did not show defects in external eye morphology or retinal cell-type specification and patterning (Figures 1C–1J and 2A–2C and not shown). We conclude that *eys* has a specific role in IRS formation during eye development.

Eys Encodes a Predicted Proteoglycan Related to Agrin and Perlecan

$eys^{BG02208}$ and eys^{G13596} carry P element insertions in the last intron of the predicted gene *CG7245* (Figure 3A; Adams et al., 2000). Northern blot analysis with a *CG7245*-specific probe identified a single transcript at embryonic, larval, and adult stages that is approximately 12 kb in length (Figure 3F), suggesting that *CG7245* (which had a predicted transcript size of 3.1 kb) represents only part of the *eys* gene. A combination of RT-PCR, 5′-RACE, and sequence analysis showed that the *eys* transcription unit extends over four predicted genes (*HDC00367*, *CG15388*, *CG15389*, and *CG7245*; Adams et al., 2000; Hild et al., 2003) and at least two additional exons (Figure 3A), and has an open reading frame encoding a product of 2176 amino acids. The protein structure of Eys is similar to many other extracellular proteins (Figure 3B). Eys contains 14 EGF (epidermal growth factor-like) domains, 4 LamG (Laminin G-like) domains, and a threonine/serine-rich region that is predicted to be highly glycosylated. This region contains consensus binding sites for glycosaminoglycans (GAG; Figures 3B and 3E; Winzen et al., 2003), suggesting that Eys may be a proteoglycan. Aside from insect orthologs of Eys and the closely related protein SP2353, we

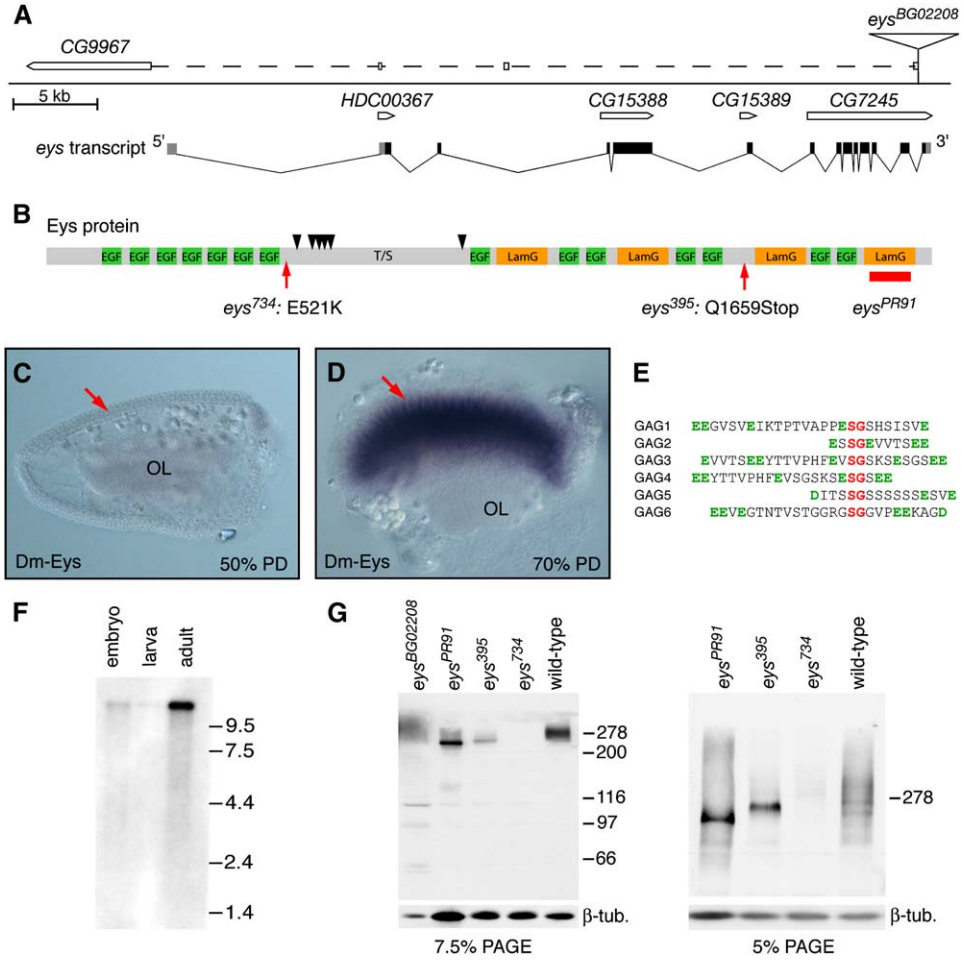

Figure 3. *eys* Structure and Expression

(A) Organization of the *eys* gene. The *eys* transcription unit comprises four predicted genes (*HDC00367*, *CG15388*, *CG15389*, and *CG7245*). The open reading frame of the *eys* transcript is shown in black. *eys* overlaps with the *CG9967* transcription unit that is read from the reverse strand. The first three predicted exons of *CG9967* are shown individually, while the remaining four are shown as a single open bar.

(B) Structure of the Eys protein. EGF domains, green; LamG domains, orange. Black triangles indicate the position of predicted GAG attachment sites within the threonine/serine (T/S)-rich region of Eys. eys^{734} is a missense mutation (E521K), eys^{395} a nonsense mutation (Q1659Stop), and eys^{PR91} is a deletion that removes exon 13 and thus most of the fourth LamG domain of Eys.

(C and D) *eys* mRNA expression in the pupal retina (red arrow). At 50% pd (C), no *eys*-specific signal is detected, whereas at 70% pd (D), high-level expression is seen in PRCs. OL, optic lobe.

(E) Alignment of predicted Eys GAG attachment sites, which are indicated by an SG sequence embedded in a region with several negatively charged amino acids (E or D). Experimentally confirmed GAG attachment sites in other proteins are often clustered, similar to sites 2–5 of Eys (Winzen et al., 2003).

(F) Northern blot analysis reveals a single *eys*-specific transcript in embryos, larvae, and adults that is approximately 12 kb in length.

(G) Immunoblot analysis of adult head lysates from wild-type and *eys* mutant animals using anti-Eys (GP5). Proteins were separated on a 7.5% or 5% SDS-PAGE gel. β-tubulin was used as a loading control. In wild-type, anti-Eys detected a high molecular weight smear that ranges in size between approximately 250 and 350 kDa.

found that Eys is most closely related to the proteoglycans agrin and perlecan among all proteins that have EGF and LamG domains, further supporting the hypothesis that Eys is a proteoglycan.

Several findings indicate that the transcription unit we characterized, and not the overlapping gene *CG9967* (Figure 3A), is *eys*. First, *eys* RNA and protein expression in PRCs are initiated at the time of IRS formation (Figures 3C, 3D, and 4A–4C), whereas *CG9967* expression was not detected in the retina. Second, eys^{PR91} contains a deletion that removes exon 13 of *eys*, leading to a predicted splice of exon 12 to exon 14 that maintains the open reading frame. This mutant splice variant would produce an Eys protein that lacks most of the fourth LamG domain (Figure 3B) and showed a strong *eys* mutant phenotype (Figures 4H and 4I). Third, sequence analysis of *eys* alleles showed that eys^{734} is a missense mutation converting a glutamic acid to lysine (E521K) and that eys^{395} is a nonsense mutation (Q1659Stop) and is therefore predicted to truncate the last 518 amino acids of Eys, removing LamG 3 and 4 and EGF 12–14 (Figure 3B). These mutations specifically affect the Eys protein, as the *eys* and *CG9967* coding regions are non-overlapping. Moreover, the analysis of eys^{PR91} suggests that the fourth LamG domain is required for Eys function in IRS formation.

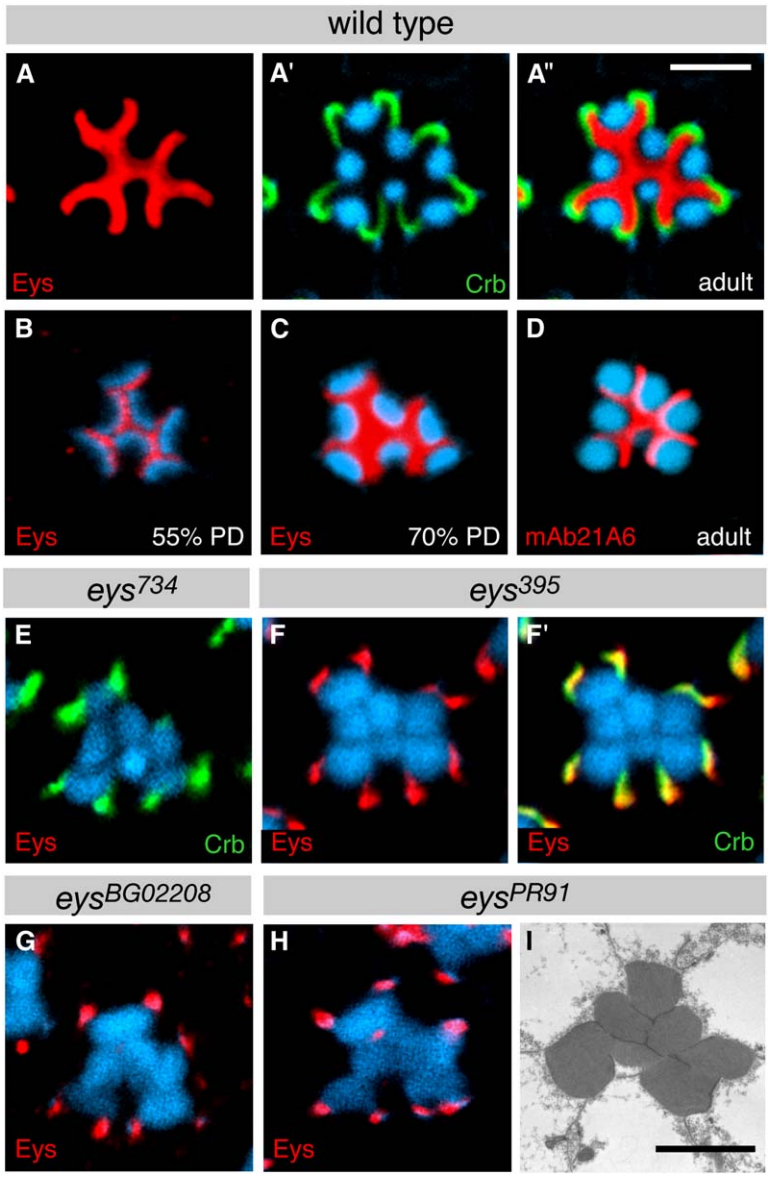

Figure 4. Eys Protein Is a Component of the IRS

(A–H) Eys is shown in red, Crumbs (Crb) in green, and rhabdomeres are labeled by staining for F-actin with phalloidin (blue).

(A–C) In wild-type, Eys was found in the IRS in adults (A), 55% pd (B), and 70% pd (C).

(D) Adult ommatidium shows mAb21A6 staining of the IRS.

(E–H) Eys labeling of *eys* mutants. eys^{734} does not show detectable levels of Eys (E). In eys^{395} (F), $eys^{BG02208}$ (G), and eys^{PR91} (H) mutants, Eys is confined to the region of the stalk membrane stained by Crumbs in (F′).

(I) TEM of eys^{PR91} mutants shows absence of IRS.

The scale bars represent (A–H) 3 μm and (I) 3 μm.

Antibodies directed against the Eys protein recognize a smear rather than discrete bands in immunoblots using adult head lysates (Figure 3G). The average molecular weight is ~280 kDa, substantially larger than the predicted molecular weight for Eys of 234 kDa. Similar high molecular weight smears were reported for proteoglycans such as agrin, and likely result from variable amounts of glycosylation (Tsen et al., 1995; Friedrich et al., 2000; Winzen et al., 2003). eys^{734} mutant animals contained little or no Eys protein, while eys^{395} mutants showed reduced amounts of Eys. The eys^{395} gene product does not show a reduction in size that would be consistent with the predicted truncation of 518 amino acids from the mutant protein. Potential explanations for this discrepancy are cryptic splicing or an altered glycosylation pattern. Cryptic splicing would remove exon 12, which contains the premature Stop codon in eys^{395} and encodes 208 amino acids. Reproducibly, we find that in lysates of eys^{395} and eys^{PR91} mutants, a major band is seen within the high molecular weight smear in contrast to wild-type, which could result from differences in gel mobility, a changed glycosylation pattern, or differential stability of Eys isoforms. Taken together, our data suggest that Eys is a proteoglycan.

Eys Is Secreted into the Interrhabdomeral Space

The *eys* mutant phenotype and the structure of the Eys protein raise the possibility that Eys is a component of the luminal matrix within the IRS. Indeed, Eys protein was localized exclusively in the IRS of adult fly retinas (Figure 4A). To determine whether Eys secretion correlates with IRS formation, we stained developing retinas. In wild-type, the IRS opens at 55% of pupal development (pd) and increases in size subsequently (Longley and Ready, 1995). Lumen staining for Eys was first seen at 55% pd and increases in intensity at later stages (Figures 4B and 4C). These findings show that Eys is an extracellular protein secreted into the IRS as it forms.

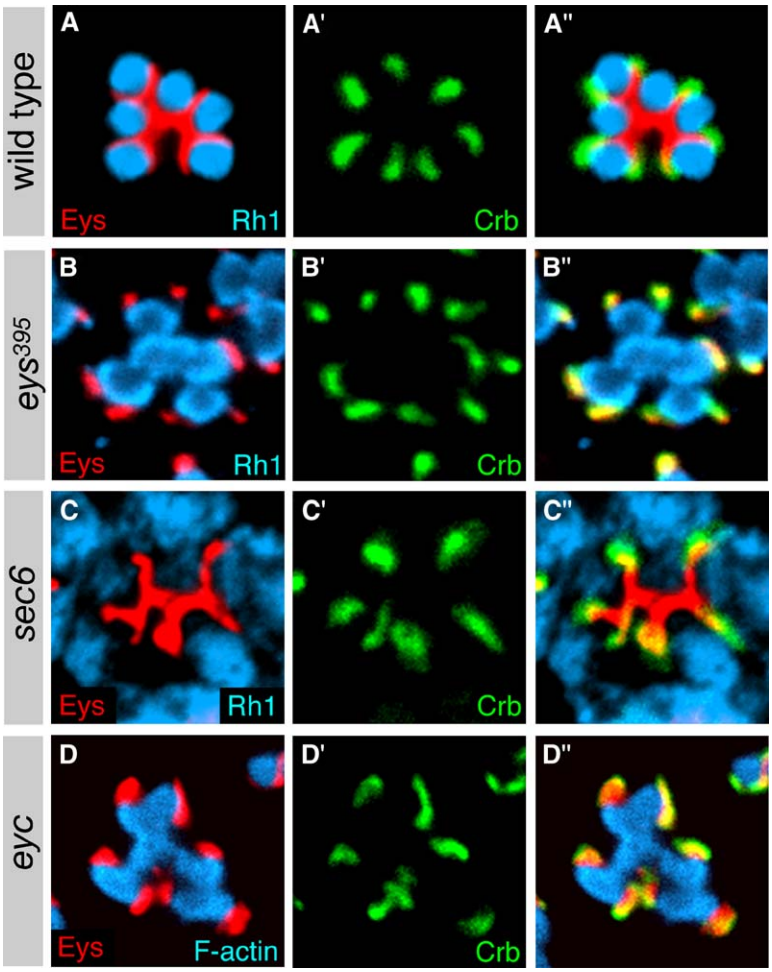

Figure 5. Eys Is Secreted through the Stalk Membrane and Expressed in *eyc* Mutants

(A–C) Wild-type (A), *eys*^{395} (B), and *sec6* (C) mutant ommatidia stained for Eys (red), Crumbs (Crb; green), and Rhodopsin 1 (Rh1; blue). Rhodopsin 1 localizes to the rhabdomeres of PRCs R1–R6 in wild-type and *eys*^{395} mutants. In contrast, Rhodopsin 1 accumulates in the cytoplasm in *sec6* mutant PRCs, whereas Eys is secreted into the IRS in this mutant.

(D) *eyc* mutant ommatidium stained for Eys (red), Crumbs (Crb; green), and F-actin (blue). The rhabdomeres remain in contact in the *eyc* mutant and Eys fills a fragmented IRS, which is present at the stalk membranes.

We also examined the formation of the IRS with the monoclonal antibody (mAb) 21A6 that was previously reported to recognize a luminal antigen in the IRS (Fujita et al., 1982; Zipursky et al., 1984). In fact, the expression profile and distribution pattern seen with mAb21A6 in wild-type and in *eys* mutants (Figure 4D; Figure S2) is identical to the pattern we found with our antibodies raised against Eys. This strongly suggests that mAb21A6 recognizes Eys.

Our immunoblot analysis indicated that the *eys* mutant alleles we analyzed still contained Eys protein. We were interested to find out how Eys is distributed in these mutants in which the IRS does not form. In *eys*^{734} mutants, Eys protein was not detected at pupal stages and in most adults (Figure 4E). Minor amounts of Eys were detected in immunoblots and occasionally seen in adult eyes, where it was confined to the stalk membrane. In *eys*^{395}, *eys*^{BG02208}, *eys*^{G13596}, and *eys*^{PR91} mutants, Eys protein was readily detected and also confined to the region of the stalk membrane, identified with the stalk marker Crumbs (Pellikka et al., 2002), and did not penetrate between rhabdomeres (Figures 4F–4H). Only in some mutant ommatidia did we detect a small amount of Eys between rhabdomeres (Figure 4H). As with Crumbs, we did not detect any defects in the distribution of several polarity markers in *eys* mutant PRCs, including the adherens junction marker DE-cadherin and the basolateral marker Na^+K^+-ATPase (Figure S3), indicating that *eys* mutants PRCs have normal epithelial polarity. Rhabdomeres were found to remain in direct contact in *eys* mutants at all stages, suggesting that the IRS never opens in animals that lack *eys* function.

Eys Is Secreted by the Stalk Membrane

Mutant Eys protein remained associated with the stalk membrane and did not penetrate between the rhabdomeres, raising the interesting possibility that Eys is specifically secreted through the stalk membrane and then spreads throughout the IRS. To test this hypothesis, we examined Eys distribution in ommatidia that lacked the function of Sec6, a component of the *Drosophila* exocyst complex that is required for targeting excretory vesicles to the rhabdomere but not the stalk or the basolateral membrane in differentiating PRCs (Beronja et al., 2005). Ommatidia with compromised Sec6 function failed to transport rhodopsin to the rhabdomere as expected but showed normal luminal deposition of Eys. Rhodopsin is delivered normally to the rhabdomere in *eys* mutants (Figures 5A–5C). These findings suggest that Eys is delivered through the stalk membrane, revealing a function for the stalk membrane in the secretion of IRS components.

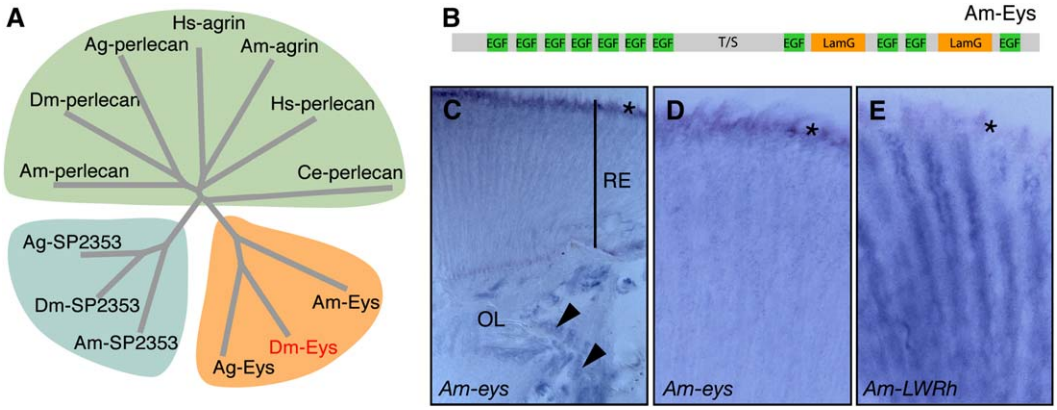

Figure 6. *Am-eys* Is Not Expressed in the Retina

(A) Phylogram of Eys and related proteins. The phylogram is based on a ClustalW alignment of LamG domains 1 and 2 and EGF domains 9–11 of Dm-Eys and the equivalent regions in all other proteins. Eys and its orthologs are closely related to a second insect-specific, and yet uncharacterized, group of predicted proteins identified by Dm-SP2353, as well as agrin and perlecan proteins from insects, nematodes, and vertebrates. Note that *A. mellifera* (Am) has a well-conserved agrin ortholog that is missing from dipterans and *C. elegans* (Ce). Ag, *A. gambiae*; Hs, *Homo sapiens*.

(B) Structure of *A. mellifera* Eys protein (Am-Eys). The distribution of EGF domains (green) and LamG domains (orange) are indicated. The Am-Eys protein is shorter than Dm-Eys, and has no predicted GAG attachment sites.

(C–E) Expression of *Am-eys* and *A. mellifera* long-wavelength Rhodopsin (*Am-LWRh*) mRNA in the late (70%–90% pd) honeybee pupal retina. Each panel shows a 20 μm thick cross-section of either the entire retina (RE) and parts of the optic lobe (OL) (C) or the distal 50% of the retina (D and E). Asterisks indicate staining in pigment cells that results from pigment granules. *Am-eys* expression is not detected in PRCs but is seen in cells of the optic lobe (arrowhead), whereas *Am-LWRh* is prominently expressed in PRCs.

Eys Acts Independently of Eyes Closed

eyes closed (*eyc*) is a previously characterized mutant that causes defects in IRS formation (Sang and Ready, 2002). *eyc* is a gain-of-function allele of the *Drosophila* p47 homolog that interferes with the recycling of apical membrane proteins such as DE-cadherin. It has been proposed that the failure of apical membranes to de-adhere as a result of DE-cadherin retention causes rhabdomeres to remain attached to each other in this mutant. A matrix-containing IRS forms, although it is fragmented and largely confined to the regions between the stalk membranes (Sang and Ready, 2002). We found that DE-cadherin is removed from the apical membrane in *eys* mutants as in wild-type (not shown). Eys was secreted in *eyc* mutants, where it filled the fragmented IRS that is associated with Crumbs-containing stalk membranes (Figure 5D). These results indicate that *eyc* and *eys* define two independent steps in IRS formation.

The *eys* Ortholog of Honeybees Is Not Expressed in PRCs

eys has well-conserved orthologs in mosquitoes (*Anopheles gambiae*; *Ag-eys*; *ENSANGG00000007435* and *ENSANGG00000024085*; Holt et al., 2002) and bees (*Apis mellifera*; *Am-eys*; *ENSAPMG00000000551*; Baylor College of Medicine, Human Genome Sequencing Center, Honey Bee Genome Project, Genome Assembly Amel 3.0, May 2005) (Figure 6A). The domain organization of Ag-Eys is similar to *D. melanogaster* Eys (Dm-Eys), whereas Am-Eys is predicted to be shorter than Dm-Eys, lacking the C-terminal region that includes LamG 3 and 4 and EGF 12–14 in Dm-Eys (compare Figures 3B and 6B). Am-Eys also lacks consensus binding sites for GAG, which are found in Dm-Eys and Ag-Eys. As the differential distribution of the Eys protein in flies is controlled at the transcriptional level as indicated by the matching distribution patterns of *eys* mRNA and protein, we speculated that in dipterans, *eys* expression was acquired by PRCs in support of IRS formation. To address this question, we examined the expression of *Am-eys*. *Am-eys* was expressed in many cells of the brain but we did not detect *Am-eys* transcript in late pupal PRCs of bee retinas, in contrast to long-wavelength rhodopsin (*Am-LWRh*; Chang et al., 1996) mRNA, which served as a positive control (Figures 6C–6E). This finding is consistent with the hypothesis that *eys* expression was recruited by PRCs in early dipteran evolution when eye structure underwent a transition from a fused to an open rhabdom configuration.

Eys Is Not Essential for Lumen Formation in Mechanosensory Organs

Eys is also expressed at low levels in the late embryonic central nervous system and in sensory organs in which Eys is confined to an apical luminal space. Both the chordotonal organs, which act as stretch receptors, and the external sensory organs, which extend a sensory hair that is responsive to touch, express *eys* transcript and protein in matching spatial and temporal cellular distributions. For example, Eys is found in the luminal space that is formed by an accessory cell around the sensory dendrite known as the scolopidium in chordotonal organs (Figures 7A–7C). The membrane of the accessory cell, the scolopale cell that surrounds the lumen, corresponds to the apical membrane of epithelial cells as indicated, for example, by the presence of the apical marker Crumbs (Figures 7A–7C). Eys is initially found along the sensory dendrite (Figure 7B). As scolopidia differentiate, Eys remains associated with the dendrite but now concentrates at the base of the scolopidium and, most prominently, in an area of the dendrite that corresponds to the ciliary dilation

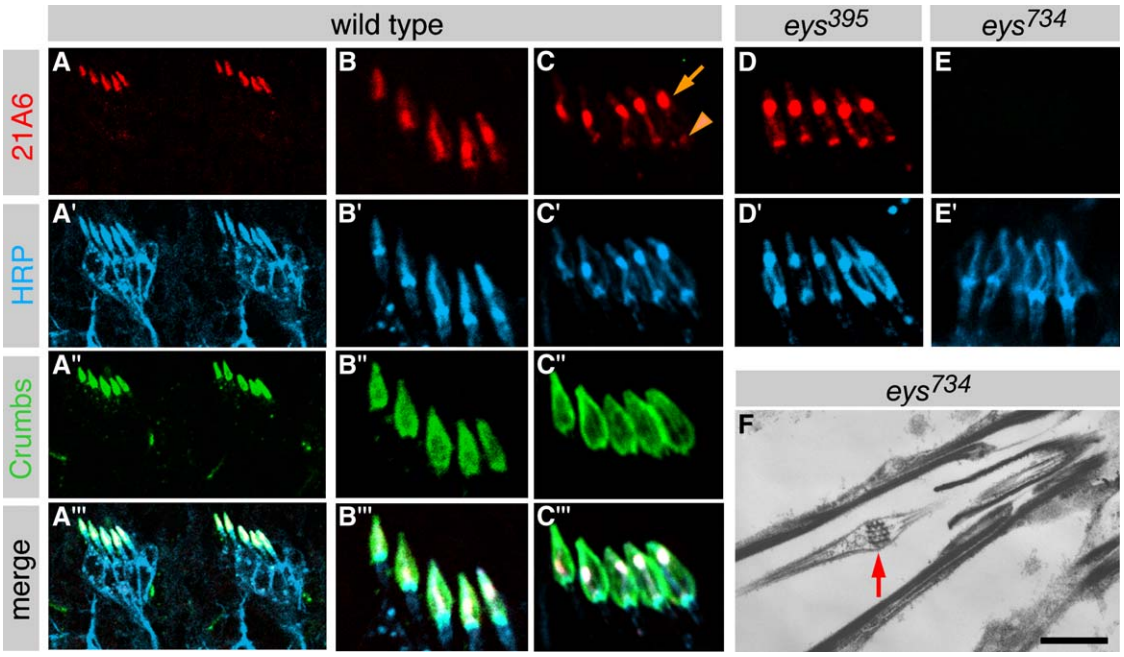

Figure 7. Eys in Mechanosensory Organs

(A) Two pentascolopidial organs in the abdomen of a *Drosophila* embryo stained for Eys (mAb21A6; red), HRP (blue), and Crumbs (green).
(B and C) Scolopidia in a stage 15 embryo (B) and a stage 17 embryo (C) labeled as in (A). Crumbs stains the membrane that surrounds the scolopidial lumen. Eys and HRP stain the sensory cilium uniformly at stage 15 (B). Both proteins accumulate at the ciliary dilation (arrow) and the base of the scolopidium (arrowhead) by stage 17.
(D) eys^{395} mutant embryo at stage 17 shows normal distribution of Eys and HRP antigen.
(E) Eys is not detectable in eys^{734} mutant embryo at stage 17 and HRP labeling fails to accumulate at the ciliary dilation.
(F) TEM of part of a scolopidium of the Johnston's organ in the second antennal segment of an eys^{734} mutant adult fly. Scolopidial ultrastructure including the ciliary dilation (arrow) is indistinguishable from wild-type (not shown). Note that axonemal microtubules bend around electron-dense material at the ciliary dilation. The scale bar represents 1 μm.

(Figure 7C), a thickening of the sensory cilium of unknown function.

eys^{395} mutants show normal levels and a normal subcellular distribution pattern of Eys (Figure 7D), while eys^{734} mutant embryos do not express detectable amounts of Eys in mechanosensory organs (Figure 7E). To counterstain neuronal membranes, we used antibodies raised against horseradish peroxidase (HRP) which appear to recognize sugar residues on multiple glycoproteins (Jan and Jan, 1982; Sun and Salvaterra, 1995; Seppo et al., 2003). Similar to Eys, anti-HRP antigens also accumulate in the ciliary dilation in wild-type and eys^{395} mutants (Figures 7B–7D). In contrast, this accumulation of HRP labeling at the ciliary dilation was not seen in eys^{734} mutants (Figure 7E), suggesting that loss of Eys leads to a molecular defect of the sensory dendrite. Ultrastructural analysis of the chordotonal organs of the Johnston's organ, which is located in the second antennal segment and aids in the detection of sound (Todi et al., 2004), did not reveal defects in chordotonal organ organization or sensory dendrite morphology in eys^{734} mutants (Figure 7F). Moreover, behavioral tests for touch sensitivity (Kernan et al., 1994) did not reveal defects in mechanoreceptor function. These observations suggest that Eys is needed for the normal distribution of anti-HRP antigens to the ciliary dilation but that the loss of Eys or the resulting defect in HRP antigen distribution does not lead to detectable changes in ultrastructure or function of mechanosensory organs.

Discussion

The formation of the IRS is a critical step in the development of a functional fly retina. Our data suggest that the secretion of the proteoglycan Eys is essential for opening up a luminal cavity between the apical membranes of PRCs. In the absence of Eys function, PRC apical membranes remain attached to each other at both the rhabdomere and the stalk membrane. Except for the lack of an IRS, PRCs appear to undergo normal differentiation including axon pathfinding. The often seen fragmentation of individual rhabdomeres into two or three blocks of microvilli may be a secondary consequence of rhabdomeres forming while they are in direct contact with rhabdomeres of other PRCs. We also detected a molecular defect in the lumen that surrounds the sensory dendrite of mechanosensory organs, although no defect in lumen integrity or mechanosensation was identified. We did not detect Eys expression in any other epithelia or lumina, suggesting that Eys plays a specific role in the formation of apical lumina of sensory epithelia.

Eys is not a component of basement membranes, like other proteoglycans, and we could not detect extracellular matrix proteins such as Laminin, Collagen IV, or Perlecan in the IRS (data not shown), suggesting that the Eys-containing apical matrix of the IRS has a composition clearly distinct from basal extracellular matrix. At present, we cannot rule out the possibility that Eys is

simply a secreted ligand that does not interact with the IRS matrix, although this seems unlikely, as Eys is distributed throughout the IRS and is not restricted to the plasma membrane. Recently, several proteins of the apical matrix, apical cell membrane, or membrane-associated cytoskeleton were shown to contribute to epithelial lumen morphogenesis of *Caenorhabditis elegans* tissues and the *Drosophila* tracheal system (Jazwinska et al., 2003; Göbel et al., 2004; Perens and Shaham, 2005; Tonning et al., 2005). Lumen morphogenesis of *Drosophila* trachea also depends on several components of the septate junction, which forms a paracellular diffusion barrier at the basolateral membrane (for a review, see Wu and Beitel, 2004). However, in all of these mutants at least some luminal space forms, suggesting that lumen formation may depend on multiple independent pathways once epithelial cells have polarized and an apical, nonadhesive membrane is established. To our knowledge, Eys is distinct from other lumen morphogenesis mutants reported, as in its absence a luminal cavity fails to form completely although epithelial polarity of PRCs is normal and the apical membranes appear intact and of normal dimensions.

Our observations suggest that Eys is secreted through the stalk membrane, as Eys remains associated with the stalk membrane in protein-positive *eys* mutants. Moreover, the loss of exocyst function, which is required for excretory vesicle delivery to the rhabdomere (Beronja et al., 2005), does not compromise Eys secretion. Modulating the length of the stalk membrane by changing the activity of Crumbs or β_H-Spectrin causes abnormalities in the dimensions of the IRS but a matrix-filled lumen forms (Pellikka et al., 2002). Interestingly, a portion of the enlarged IRS that forms as a result of Crumbs overexpression is often not filled with matrix as detected by transmission electron microscopy (TEM), and the matrix remains attached to the distended apical membrane, leaving an empty central space. This suggests that the IRS does not have to be filled with matrix throughout to maintain an open lumen.

We hypothesize that the recruitment of *eys* expression by dipteran PRCs was an important element in the transition from the ancestral apposition compound eye to the neural superposition eye of flies. The *eys* ortholog of *A. gambia* is well conserved. Many mosquito species display an IRS similar to flies, whereas *A. gambia* has a highly modified ommatidial structure that is adapted to nocturnal vision (Land et al., 1999). In contrast, *A. mellifera* ommatidia do not show an IRS, and honeybees have an Eys ortholog that apparently lacks potential GAG attachment sites and some protein domains compared to the fly and mosquito proteins. Dipterans have orthologs of perlecan but not of agrin, raising the possibility that Eys is a modified version of agrin. This seems unlikely, however, as the bee genome encodes well-conserved perlecan and agrin orthologs in addition to Am-Eys. As we did not find a clear *eys* ortholog in genomes of animals outside the insects, we speculate that *eys* (as well as the closely related gene *SP2353*) may have arisen through gene duplication from either agrin or perlecan genes. Interestingly, bee PRCs lack stalk membranes, raising the possibility that stalk membranes, through which Eys is secreted, and the IRS matrix may have coevolved.

The creation of a luminal space often goes hand in hand with cell polarization and apical membrane formation (O'Brien et al., 2002; Lubarsky and Krasnow, 2003). In *Drosophila* PRC differentiation, these processes are temporally separated, allowing individual aspects of lumen formation to be analyzed independently. In addition to de-adhesion of apical membranes (Sang and Ready, 2002), secretion of Eys through the stalk membrane into the IRS is required to open a luminal space. Water import may play an important role in generating a luminal cavity in tissues such as the lung epithelia, which seems to be caused by an ionic gradient that generates osmotic pressure (reviewed in Lubarsky and Krasnow, 2003). As a highly glycosylated proteoglycan, Eys could promote lumen expansion by attracting water (Wight et al., 1991). However, such a simple model for Eys function is not supported by our observation that an Eys protein that lacks only the fourth LamG domain and remains glycosylated, as suggested by our immunoblot analysis, is secreted normally but remains at the stalk and is incapable of opening a lumen. Some of the C-terminal LamG and EGF domains in agrin and perlecan are known to interact with cellular receptors such as dystroglycan and integrin (reviewed in Bezakova and Ruegg, 2003). Interaction of Eys with a receptor could promote its spreading from the stalk to the rhabdomere to fill the IRS. Alternatively, this interaction could elicit a cellular response that is essential for IRS formation, such as the secretion of additional lumen components.

Experimental Procedures

Insect Strains

Drosophila melanogaster eys^{734} and eys^{395} were isolated in an ethane methyl sulfonate mutagenesis screen (Clandinin et al., 2001). Both *eys* alleles failed to complement *Df(2L)BSC37* (22D2-3;22F1-2). $eys^{BG02208}$ was obtained from the Bloomington *Drosophila* Stock Center, and eys^{G13596} from Genexel. Mobilization of $eys^{BG02208}$ generated 38 additional *eys* alleles by imprecise excisions including eys^{PR91}. PCR analysis showed that eys^{PR91} contains a deletion of exon 13. The predicted splice from exon 12 to exon 14 maintains the open reading frame, giving rise to an Eys protein that lacks amino acids 1949–2114. The eyc^{1} strain is described in Sang and Ready (2002). Generation of *sec6* mutant eye clones is described in Beronja et al. (2005). The wild-type strain used was OregonR. *Apis mellifera*: adult and late pupal stage honeybees (workers and drones) were obtained from local beekeepers Horst Goelder (Kortright Centre) and Ellen Larsen. Pupal staging was according to cuticle pigmentation.

Antibody Production

A 600 bp fragment encoding amino acids 227–426 of Eys was ligated into pGEX-6-P1 (Amersham Biosciences). Fusion protein was purified using standard methods, and antibodies were raised in guinea pigs.

Immunostainings and Transmission Electron Microscopy

The following primary antibodies were used: guinea pig polyclonal antibody (pAb) anti-Eys (GP5); mouse mAb21A6 (Zipursky et al., 1984); rat mAb anti-DE-cadherin (Oda et al., 1994); rabbit pAb anti-Rh1 (Satoh et al., 2005); mouse mAb anti-Rh1 (Kumar and Ready, 1995); rat pAb anti-Crb (Pellikka et al., 2002); mAb24B10 (anti-Chaoptin; Zipursky et al., 1984); guinea pig anti-BSH (Poeck et al., 2001); rat anti-Elav; mouse mAb6H4 and mouse anti-Na^+K^+-ATPase (Developmental Studies Hybridoma Bank); and mouse anti-β-Gal (Promega). Anti-HRP was conjugated to Cy3 (Jackson ImmunoResearch). Secondary antibodies were conjugated with Alexa 488, Alexa 594 (Molecular Probes), Cy3, or Cy5 (Jackson ImmunoResearch). F-actin was stained with Alexa Fluor 488-phalloidin (Molecular Probes). Pupal and adult retinas were staged at 25°C, dissected

in phosphate buffer (PB), fixed in 4% formaldehyde in PB, and stained as previously reported (Clandinin et al., 2001; Pellikka et al., 2002). Confocal images were taken on a Carl Zeiss LSM510 or Leica TCS SP2 AOBS. Images were processed in Adobe Photoshop and Adobe Illustrator. TEM preparations were carried out as described (Pellikka et al., 2002).

Western Blot Analysis

Adult heads were homogenized in SDS sample buffer (62.5 mM Tris-HCl [pH 6.8], 2.3% SDS, 10% glycerol, 5% β-mercaptoethanol, and 0.005% bromphenol blue). Fifty micrograms of proteins were separated by 5% or 7.5% SDS-PAGE and electrotransferred onto nitrocellulose membranes (Amersham Biosciences) as described in Beronja et al. (2005). The following primary antibodies were used: mouse anti-β-tubulin (mAbE7); mouse pAb anti-α-spectrin (3A9) (Developmental Studies Hybridoma Bank); and guinea pig pAb anti-Eys (GP5).

Molecular Biology

Oligonucleotide primers used in this study are listed in Table S1. A combination of RT-PCR and 5′-RACE (GeneRacer, Invitrogen), together with *D. melanogaster* adult poly-(A+) RNA (Clontech), was used to characterize the *eys* transcript. We amplified a 1608 bp fragment that contains the *eys* start codon and 870 bp of 5′-UTR. Systematic RT-PCR and sequencing identified exon-intron boundaries. Together, this analysis identified a 7705 bp long transcript that contained an open reading frame of 6528 bp. As the 3′-UTR of *eys* is contained within the partial cDNA clone HL01481, it is likely that the missing sequence of the *eys* transcript is part of an extensive 5′-UTR. RT-PCR analysis did not reveal the presence of alternative splice products, consistent with our Northern blot data. A poly-(A+) Northern blot (a gift of Sabrina Kim and Gabrielle Boulianne) was probed with a 236 bp EcoRI/KpnI fragment of *eys* cDNA clone HL01481 and a 498 bp genomic fragment contained within exon 5 (previously *CG15388*) of *eys* (Figure 3A). Whole-mount in situ hybridization on fly and bee pupal retinas followed established protocols (Tautz and Pfeifle, 1989) using random-primed digoxygenin-labeled DNA probes (Roche). *eys*-specific probes were the cDNA clone HL01481 that covers part of *CG7245*, a genomic 558 bp fragment of *CG7245*, a 498 bp fragment of *CG15388*, and a 278 bp fragment of *CG15389*. All *eys*-specific probes revealed a similar expression pattern. cDNA clone LD01251 was labeled to generate a *CG9967*-specific probe. To generate *Am-eys*-specific probes, we used three genomic fragments of 1758 bp, 879 bp, and 1256 bp that together cover most of the *Am-eys* transcript. The *Am-LWRh* probe was a 1188 bp genomic fragment.

Touch Sensitivity Assay

Touch sensitivity was tested on single foraging third-instar larvae (either 80 hr or 96 hr after egg laying) at 25°C as described in Kernan et al. (1994) with minor modifications—each larva was touched and scored three times, with a range of possible scores from 0 to 12. Larvae were handled as described in Caldwell et al. (2003). All lines were coded for an unbiased scoring of individual larvae.

Supplemental Data

Supplemental Data include three figures and one table and are available at http://www.developmentalcell.com/cgi/content/full/11/4/483/DC1/.

Acknowledgments

We thank Seymour Benzer, Don Ready, Sabrina Kim, Gabrielle Boulianne, Horst Goelder, Ellen Larsen, the Developmental Studies Hybridoma Bank, the Bloomington *Drosophila* Stock Center, and the *Drosophila* Genomic Resource Center for fly stocks, bees, and reagents. We thank Dorothea Godt for discussion and critical comments on the manuscript and Andrew Zelhof for discussing data prior to publication. This work was supported by a predoctoral fellowship of the Vision Research Program, University of Toronto (N.H.), and grants from the National Institutes of Health, USA (R01, EY015231-01A1; T.R.C.) and the National Science and Engineering Research Council, Canada (U.T.).

Received: December 30, 2005
Revised: June 26, 2006
Accepted: August 17, 2006
Published: October 2, 2006

References

Adams, M.D., Celniker, S.E., Holt, R.A., Evans, C.A., Gocayne, J.D., Amanatides, P.G., Scherer, S.E., Li, P.W., Hoskins, R.A., Galle, R.F., et al. (2000). The genome sequence of *Drosophila melanogaster*. Science *287*, 2185–2195.

Affolter, M., Bellusci, S., Itoh, N., Shilo, B., Thiery, J.P., and Werb, Z. (2003). Tube or not tube: remodeling epithelial tissues by branching morphogenesis. Dev. Cell *4*, 11–18.

Beronja, S., Laprise, P., Papoulas, O., Pellikka, M., Sisson, J., and Tepass, U. (2005). Essential function of *Drosophila* Sec6 in apical exocytosis of epithelial photoreceptor cells. J. Cell Biol. *169*, 635–646.

Bezakova, G., and Ruegg, M.A. (2003). New insights into the roles of agrin. Nat. Rev. Mol. Cell Biol. *4*, 295–308.

Braitenberg, V. (1967). Patterns of projection in the visual system of the fly. I. Retina-lamina projections. Exp. Brain Res. *3*, 271–298.

Caldwell, J.C., Miller, M.M., Wing, S., Soll, D.R., and Eberl, D.F. (2003). Dynamic analysis of larval locomotion in *Drosophila* chordotonal organ mutants. Proc. Natl. Acad. Sci. USA *100*, 16053–16058.

Chang, B.S., Ayers, D., Smith, W.C., and Pierce, N.E. (1996). Cloning of the gene encoding honeybee long-wavelength rhodopsin: a new class of insect visual pigments. Gene *173*, 215–219.

Clandinin, T.R., Lee, C.H., Herman, T., Lee, R.C., Yang, A.Y., Ovasapyan, S., and Zipursky, S.L. (2001). LAR regulates R1–R6 and R7 target specificity in the visual system. Neuron *32*, 237–248.

Colas, J.F., and Schoenwolf, G.C. (2001). Towards a cellular and molecular understanding of neurulation. Dev. Dyn. *221*, 117–145.

Devine, W.P., Lubarsky, B., Shaw, K., Luschnig, S., Messina, L., and Krasnow, M.A. (2005). Requirement for chitin biosynthesis in epithelial tube morphogenesis. Proc. Natl. Acad. Sci. USA *102*, 17014–17019.

Friedrich, M.V., Schneider, M., Timpl, R., and Baumgartner, S. (2000). Perlecan domain V of *Drosophila melanogaster*. Sequence, recombinant analysis and tissue expression. Eur. J. Biochem. *267*, 3149–3159.

Fujita, S.C., Zipursky, S.L., Benzer, S., Ferrus, A., and Shotwell, S.L. (1982). Monoclonal antibodies against the *Drosophila* nervous system. Proc. Natl. Acad. Sci. USA *79*, 7929–7933.

Göbel, V., Barrett, P.L., Hall, D.H., and Fleming, J.T. (2004). Lumen morphogenesis in *C. elegans* requires the membrane-cytoskeleton linker *erm-1*. Dev. Cell *6*, 865–873.

Gonzalez-Fernandez, F. (2003). Interphotoreceptor retinoid-binding protein—an old gene for new eyes. Vision Res. *43*, 3021–3036.

Hemphälä, J., Uv, A., Cantera, R., Bray, S., and Samakovlis, C. (2003). Grainy head controls apical membrane growth and tube elongation in response to Branchless/FGF signalling. Development *130*, 249–258.

Hild, M., Beckmann, B., Haas, S.A., Koch, B., Solovyev, V., Busold, C., Fellenberg, K., Boutros, M., Vingron, M., Sauer, F., et al. (2003). An integrated gene annotation and transcriptional profiling approach towards the full gene content of the *Drosophila* genome. Genome Biol. *5*, R3.

Hogan, B.L., and Kolodziej, P.A. (2002). Organogenesis: molecular mechanisms of tubulogenesis. Nat. Rev. Genet. *3*, 513–523.

Holt, R.A., Subramanian, G.M., Halpern, A., Sutton, G.G., Charlab, R., Nusskern, D.R., Wincker, P., Clark, A.G., Ribeiro, J.M., and Wides, R. (2002). The genome sequence of the malaria mosquito *Anopheles gambiae*. Science *298*, 129–149.

Jan, L.Y., and Jan, Y.N. (1982). Antibodies to horseradish peroxidase as specific neuronal markers in *Drosophila* and in grasshopper embryos. Proc. Natl. Acad. Sci. USA *79*, 2700–2704.

Jazwinska, A., Ribeiro, C., and Affolter, M. (2003). Epithelial tube morphogenesis during *Drosophila* tracheal development requires Piopio, a luminal ZP protein. Nat. Cell Biol. *5*, 895–901.

Kernan, M., Cowan, D., and Zuker, C. (1994). Genetic dissection of mechanosensory transduction: mechanoreception-defective mutations of *Drosophila*. Neuron *12*, 1195–1206.

Kirschfeld, K. (1967). The projection of the optical environment on the screen of the rhabdomere in the compound eye of the Musca. Exp. Brain Res. *3*, 248–270.

Kumar, J.P., and Ready, D.F. (1995). Rhodopsin plays an essential structural role in *Drosophila* photoreceptor development. Development *121*, 4359–4370.

Land, M.F., and Nilsson, D.-E. (2002). Animal Eyes (Oxford: Oxford University Press).

Land, M.F., Gibson, G., Horwood, J., and Zeil, J. (1999). Fundamental differences in the optical structure of the eyes of nocturnal and diurnal mosquitoes. J. Comp. Physiol. [A] *185*, 91–103.

Longley, R.L., Jr., and Ready, D.F. (1995). Integrins and the development of three-dimensional structure in the *Drosophila* compound eye. Dev. Biol. *171*, 415–433.

Lubarsky, B., and Krasnow, M.A. (2003). Tube morphogenesis: making and shaping biological tubes. Cell *112*, 19–28.

Moussian, B., Tang, E., Tonning, A., Helms, S., Schwarz, H., Nusslein-Volhard, C., and Uv, A.E. (2005). *Drosophila* Knickkopf and Retroactive are needed for epithelial tube growth and cuticle differentiation through their specific requirement for chitin filament organization. Development *133*, 163–171.

Myat, M.M., and Andrew, D.J. (2002). Epithelial tube morphology is determined by the polarized growth and delivery of apical membrane. Cell *111*, 879–891.

O'Brien, L.E., Zegers, M.M., and Mostov, K.E. (2002). Building epithelial architecture: insights from three-dimensional culture models. Nat. Rev. Mol. Cell Biol. *3*, 531–537.

Oda, H., Uemura, T., Harada, Y., Iwai, Y., and Takeichi, M. (1994). A *Drosophila* homolog of cadherin associated with armadillo and essential for embryonic cell-cell adhesion. Dev. Biol. *165*, 716–726.

Pellikka, M., Tanentzapf, G., Pinto, M., Smith, C., McGlade, C.J., Ready, D.F., and Tepass, U. (2002). Crumbs, the *Drosophila* homologue of human CRB1/RP12, is essential for photoreceptor morphogenesis. Nature *416*, 143–149.

Perens, E.A., and Shaham, S. (2005). *C. elegans daf-6* encodes a patched-related protein required for lumen formation. Dev. Cell *8*, 893–906.

Poeck, B., Fischer, S., Gunning, D., Zipursky, S.L., and Salecker, I. (2001). Glial cells mediate target layer selection of retinal axons in the developing visual system of *Drosophila*. Neuron *29*, 99–113.

Sang, T.K., and Ready, D.F. (2002). Eyes closed, a *Drosophila* p47 homolog, is essential for photoreceptor morphogenesis. Development *129*, 143–154.

Satoh, A.K., O'Tousa, J.E., Ozaki, K., and Ready, D.F. (2005). Rab11 mediates post-Golgi trafficking of rhodopsin to the photosensitive apical membrane of *Drosophila* photoreceptors. Development *132*, 1487–1497.

Schmitz, B., Papan, C., and Campos-Ortega, J.A. (1993). Neurulation in the anterior trunk region of the zebrafish *Brachydanio rerio*. Rouxs Arch. Dev. Biol. *202*, 250–259.

Seppo, A., Matani, P., Sharrow, M., and Tiemeyer, M. (2003). Induction of neuron-specific glycosylation by Tollo/Toll-8, a *Drosophila* Toll-like receptor expressed in non-neural cells. Development *130*, 1439–1448.

Sun, B., and Salvaterra, P.M. (1995). Two *Drosophila* nervous system antigens, Nervana 1 and *2*, are homologous to the β subunit of Na^+K^+-ATPase. Proc. Natl. Acad. Sci. USA *92*, 5396–5400.

Tautz, D., and Pfeifle, C. (1989). A non-radioactive in situ hybridization method for the localization of specific RNAs in *Drosophila* embryos reveals translational control of the segmentation gene hunchback. Chromosoma *98*, 81–85.

Todi, S.V., Sharma, Y., and Eberl, D.F. (2004). Anatomical and molecular design of the *Drosophila* antenna as a flagellar auditory organ. Microsc. Res. Tech. *63*, 388–399.

Tonning, A., Hemphälä, J., Tang, E., Nannmark, U., Samakovlis, C., and Uv, A. (2005). A transient luminal chitinous matrix is required to model epithelial tube diameter in the *Drosophila* trachea. Dev. Cell *9*, 423–430.

Tsen, G., Halfter, W., Kroger, S., and Cole, G.J. (1995). Agrin is a heparan sulfate proteoglycan. J. Biol. Chem. *270*, 3392–3399.

Wight, T.N., Heinegard, D.K., and Hascall, V.C. (1991). Proteoglycans: structure and function. In Cell Biology of Extracellular Matrix, E.D. Hay, ed. (New York: Plenum Press), pp. 45–71.

Winzen, U., Cole, G.J., and Halfter, W. (2003). Agrin is a chimeric proteoglycan with the attachment sites for heparan sulfate/chondroitin sulfate located in two multiple serine-glycine clusters. J. Biol. Chem. *278*, 106–114.

Wu, V.M., and Beitel, G.J. (2004). A junctional problem of apical proportions: epithelial tube-size control by septate junctions in the *Drosophila* tracheal system. Curr. Opin. Cell Biol. *16*, 493–499.

Zipursky, S.L., Venkatesh, T.R., Teplow, D.B., and Benzer, S. (1984). Neuronal development in the *Drosophila* retina: monoclonal antibodies as molecular probes. Cell *36*, 15–26.

Accession Numbers

The GenBank accession number of eys is DQ991915.